Effect of Blade Angle on Aerodynamic Performance of Archimedes Spiral Wind Turbine

Andrew Maher Labib[1,*], Ahmed Farouk Abdel Gawad[1], Mofreh Melad Nasseif[1]

1   Mechanical Power Engineering Deptartment, Faculty of Engineering, Zagazig University, Zagazig 44519, Egypt

ARTICLE INFO	ABSTRACT
	Energy harvesting from wind in urban areas is an important solution to meet energy needs and environmental care. This study describes the effect of blade angle on the aerodynamic performance of small-scale Archimedes spiral-wind-turbine blades by computational simulation, which is experimentally validated. Archimedes wind turbine is classified as one of the HAWTs. The computational approach was used to predict the aerodynamic performance of the scaled-down rotor blades. Blade angle is defined by the angle between the rotational axis and the tip of the blade, which varied from 50° to 65° with an interval of 5°. The computational study was carried out using the ANSYS CFX 19 software for a steady incompressible flow. The performance parameters of the wind turbine, which are power and torque coefficients were explored for different blade angles. This was carried out for wind speed from 5 to 12 m/s with an interval of 1 m/s. In order to validate the results of the computational simulation, an experimental study was carried out using a scaled-down 3D-printed models. The experimental study concentrated on the effect of blade angle on the rotating speed for the different turbine models. Obviously, the results highlight that the maximum power coefficient has an inverse relation to the blade angle.

1. Introduction

Wind is one of the cleanest types of renewable energy that does not produce neither air nor water pollution. Wind turbines are classified into two major types HAWT and VAWT, which are Horizontal-Axis Wind Turbine and Vertical-Axis Wind Turbine, respectively. For large wind turbines, the traditional horizontal-axis lift type wind turbines with three blades has the highest aerodynamic efficiency. Small-size wind turbines can be classified by the type of the effective aerodynamic force that acts on the turbine blades; either lift or drag.

Many investigations were performed to study and compare the performance of HAWTs and VAWTs either separately or combined. Paraschivoiu *et al.,* [1] performed an analytical study on

---

output power of HAWT and VAWT. They found that, at 15% lower rated wind speed, VAWT delivers 41% higher power coefficient (C_p) compared to HAWT. Johari *et al.,* [2] investigated experimentally the performance of 3-bladed HAWT, and Darrieus-type VAWT. Their HAWT generated higher voltage up to 8.99V and VAWT generated only 1.4 V, however, with changing of wind direction the HAWT decreased to 0.0V while the VAWT output did not change at all. Pope *et al.,* [3] performed an energy and exergy analysis on four different turbines; two HAWTs of traditional airfoils and two VAWTs of Savonius and Zephyr turbines. Galinos *et al.,* [4] studied the capability of wind turbine minimum design requirements in the case of an onshore Darrieus VAWT and compared the results of basic Design Load Cases (DLCs) with those of 3-bladed HAWT. Govind [5] investigated the combined 12-KW NREL-Phase VI HAWT and 10-KW NACA0021 H-rotor VAWT systems by coupling their drivetrain system by a continuous variable transmission (CVT). Govind's study included the concept of motion transfer and a CFD investigation to confirm the ability of aerodynamic performance of the combined system. For HAWT, Khaled *et al.,* [6] studied numerically and experimentally the effect of different configuration of winglet on aerodynamic performance of NACA4412-bladed HAWT. Power coefficient increased by 8.787% compared to traditional HAWT. Chen *et al.,* [7] performed design and dynamic analysis of 400W SD-8000 bladed HAWT and axial-flux permanent magnet generator using GUI software to get the optimum design point for the whole system. For VAWT, Tjahjana *et al.,* [8] improved the power coefficient of Savonius wind turbine by 21.46% by using Omni-Directional Guide Vanes (ODGV). Jang *et al.,* [9] numerically predicted the performance of Savonius wind turbine and experimentally validated the results. The maximum power coefficient was 0.17 at tip-speed ratio of 0.54.

Archimedes wind turbine is one type of the horizontal-axis turbines. However, there is a difference between the Archimedes design and the traditional HAWT models. Unlike the traditional HAWTs, which use the lift force to generate power from wind energy, the Archimedes spiral-wind-turbines use both the lift and drag forces. Another difference between Archimedes turbines and traditional turbines is the direction of the flow, in traditional turbines the flow enters and exits from the same direction but in Archimedes turbine the flow enters axially and exits radially by nature due to the shape of the blade. Some researchers investigated the changing of flow direction on aerodynamic performance of traditional VAWT by artificial methods like external casing. Loganathan *et al.,* [10] studied experimentally the effect of cowling device on 8 and 16 semicircular shaped bladed VAWT to exit the flow axially. Cowling device increased the rotor speed of the 16-bladed model by 26% and the 8-bladed model by 40%. Sometimes the spiral principle used in Archimedes wind turbine is employed in the casing of the cowling device rather than the rotor. Gürbüz *et al.,* [11] investigated computationally (2D) the effect of changing the flow direction by spiral casing on different 6 models with different spiral casings. In Gürbüz's model, the flow enters radially and exits axially from both sides of the turbine. Acarer *et al.,* [12] continued Gürbüz's [11] work by making a design exploration over the complex 3D flow-field of the turbine with pursued by machine learning algorithms coupled with CFD simulations.

Archimedes wind-turbine blades follow the wind direction automatically because the yaw is passively directed due to the drag force. Another advantage is the low noise-level because of the relatively low operating-rotational-speed.

To overcome the limitation of HAWT in urban environment and the low efficiency of VAWT, Mieremet invented the Archimedes spiral wind turbine and discussed its advantages as mentioned in [13].

Many investigations were carried out by other researchers who considered the performance characteristics of the Archimedes wind-turbines.

Lu *et al.,* [14] invented a theoretical output-prediction-model of spiral wind turbines based on the angular momentum equation. Also, they performed a CFD simulation of a full-scale 0.5 kW-model with 1.5 m-diameter to predict the wind turbine performance. Thus, they compared the results of both the proposed theoretical model and CFD simulation. Based on their two techniques, they stated that the power coefficient, which referred to the mechanical efficiency, of their Archimedes spiral wind-turbine was 0.25. Safdari, and Kim [15] created a scaled-model Archimedes wind-turbine to analyze numerically its aerodynamic characteristics. Kim *et al.,* [16-18] studied three cases of 1/10 down-scale models of an Archimedes wind-turbine of 0.5 kW. For all the investigations [15-18], experimental validation was conducted for flow characterization around the rotor using PIV measurements. Furthermore, Ji *et al.,* [19] and Li *et al.,* [20] investigated the effect of both the wind direction, and angle of attack on the flow characteristics using PIV method. Yang *et al.,* [21] invented the first method for the turbine mass production. Ji *et al.,* [22,23] studied experimentally the aerodynamic performance of a full-scale Archimedes wind-turbine of 0.5 kW using two types of wind tunnel with two different cross-sectional areas. Chaudhary *et al.,* [24] designed full-scale Archimedes models for both numerical and experimental investigations. Sandeep *et al.,* [25] and Rao *et al.,* [26] modified the turbine-blade shape using NACA 2412, and NACA 6409 airfoils. Ebrahimi, and Ghassemi [27] investigated numerically the aerodynamic performance for the full-scale, and 1/10 down-scale Archimedes models with different pitch angles. Jang *et al.,* [28] extended the numerical and experimental investigation of the aerodynamic performance of the full-scale Archimedes turbines with different dimensions.

The above literature review demonstrates the real need for further investigation about the effect of blade angle on the aerodynamic performance of the Archimedes spiral wind-turbine. Thus, Figure 1 shows the schematic diagram of 1/10 down-scale model of 0.5 kW-turbine, which was numerically and experimentally investigated in the present study. Actually, the geometry of the spiral blades was considered as a great challenge. The investigated model had a diameter of 0.15 m and an aspect ratio (diameter/length) of 1.5. Thus, according to the traditional Archimedes wind-turbine-blades patent [29], the length of the turbine blade was 0.1 m. The blade angle (γ) is defined as the angle between the tip of the blade and the horizontal axis from the front side as shown in Figure 1. In the present work, the blade angle was studied at 50°, 55°, 60°, and 65°.
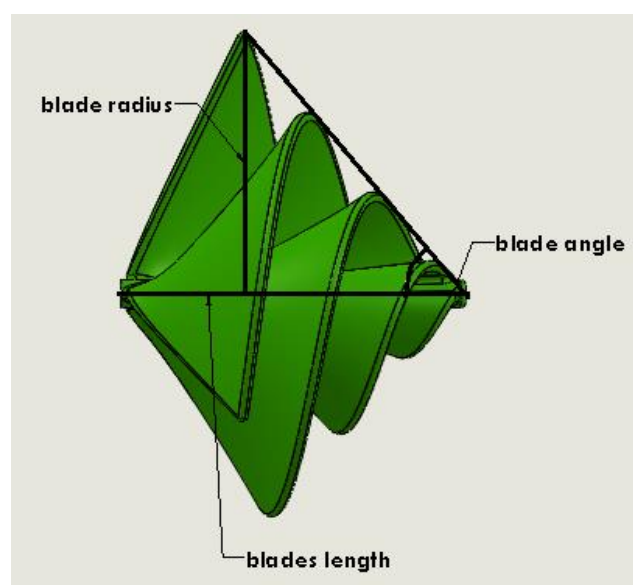

Fig. 1. Schematic diagram of the geometric parameters of the Archimedes turbine blades

The present study investigates the aerodynamic performance of the small-scale Archimedes spiral wind turbines computationally and experimentally in a wind tunnel. Hereby is another literature review concerning the methods and parameters used in studying the small-scale turbines computationally and experimentally. Rozaim *et al.,* [30] used a developed test rig to evaluate electric generation of a small-scale wind turbine. Majunit *et al.,* [31] studied numerically the effect of vortex around the wind turbine blade with a model of cambered thin plate (8312) on aerodynamic efficiency at low wind-speed for single rotor and interaction of upstream and downstream of two rotors. Gahraz *et al.,* [32] studied the wind turbine airfoil FFA-W-3-270 in a wind tunnel with zigzag tape. Khanjari *et al.,* [33] used both computational fluid dynamics (CFD) and user-defined-function (UDF) code, and also the actuator disc model in both wind tunnel and free-stream to study the effect of metrological variables like ambient pressure, temperature, velocity, and specific humidity. The maximum difference between wind tunnel and free-stream results of exergy efficiency at 16 m/s was 7.01%. Xu *et al.,* [34] performed numerical simulation and wind tunnel test on disc-shaped wind rotor to study the influencing factors on small-scale wind turbines.

2. Methodology
2.1 Computational Study

Four 3D models of the Archimedes wind turbine were developed using SolidWorks software version 2018 at the different four blade angles (50°, 55°, 60°, 65°) as shown in Figure2.
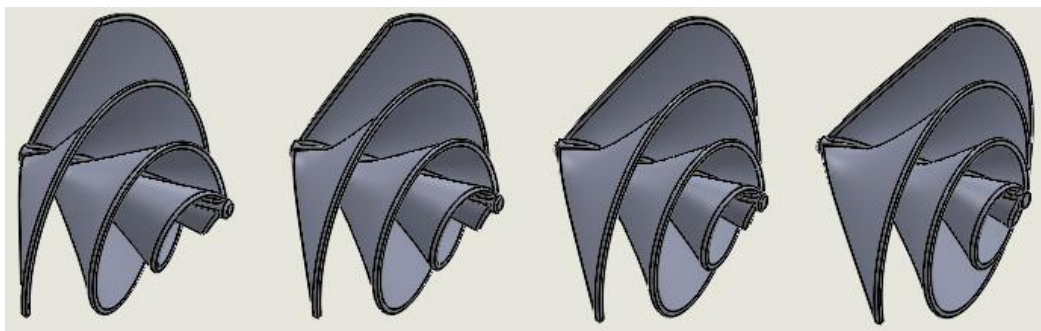
**Fig. 2.** Present four 3D models of Archimedes wind turbine

CFD investigation was carried out using ANSYS CFX version 19.0 [14, 16-18, 24, 27]. Figure 3 shows the overall computational domain, which includes the inner rotating domain of the Archimedes wind turbine and the outer stationary domain of the flow field, which was set to 0.4 × 0.4 m² [16-18]. Consequently, the blockage ratio of the frontal area was 11.0%. A previous investigation [35] suggested that the blockage ratio, based on the frontal area, should be less than 14%. Thus, the effect of the blockage ratio is negligible for the present study. The overall length of the outer stationary domain was set as 1.5 m, which is 10 times the turbine diameter to ensure flow demonstration at the outlet section of the computational domain [16-18]. The turbine was located at 2.5 times the rotor diameter from the domain inlet.

As can be seen in Figure 3, the design wind speed (U) of 5 m/s was set at the inlet boundary. At the outlet boundary, gauge pressure (zero Pa) was applied for the four turbine models [14-18,24,26,28]. The tip-speed ratio varied between 0.15 and 3.29, consequently, fifteen cases for each model were solved at U = 5 m/s. Free-slip boundaries were applied to the four side surfaces of the stationary domain [16].
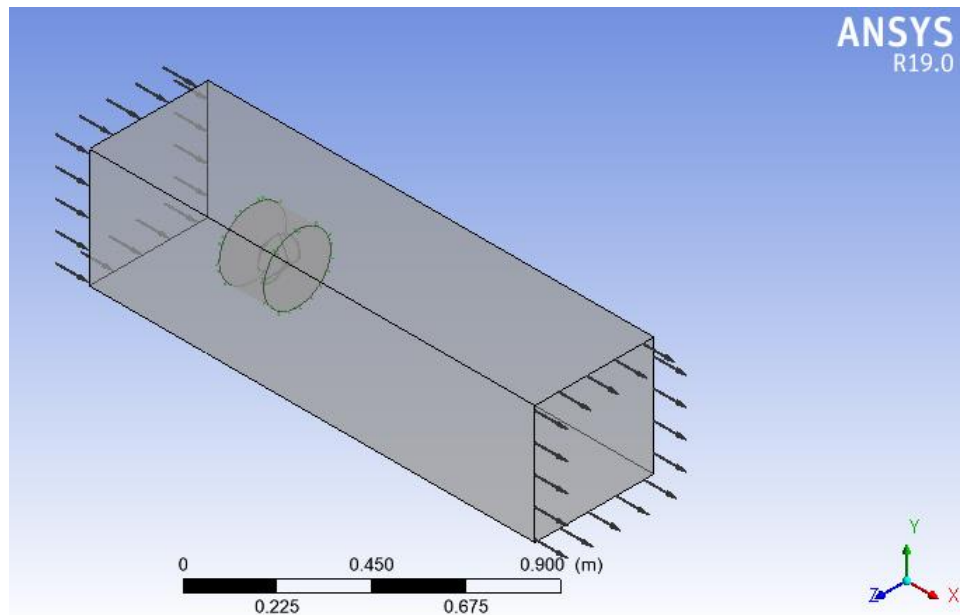
Fig. 3. Inner rotating domain of the Archimedes wind turbine, and the outer stationary domain with boundary conditions

Figure 4 illustrates the computational mesh, which was consisted of tetrahedral elements to save computational run-time [14,16-18,24,27,28]. The smallest dimension of the mesh element at the turbine face was set to be 3 mm, which was equal to the minimum thickness of the rotor blades. The first layer-height of the mesh was set to 0.1 mm to ensure that the value of Y^+ next to the blade to be approximately 4 [16,27]. The mesh size at the interface between the rotating and stationary domains was set to 5 mm to give a continuous and homogeneous flow field.
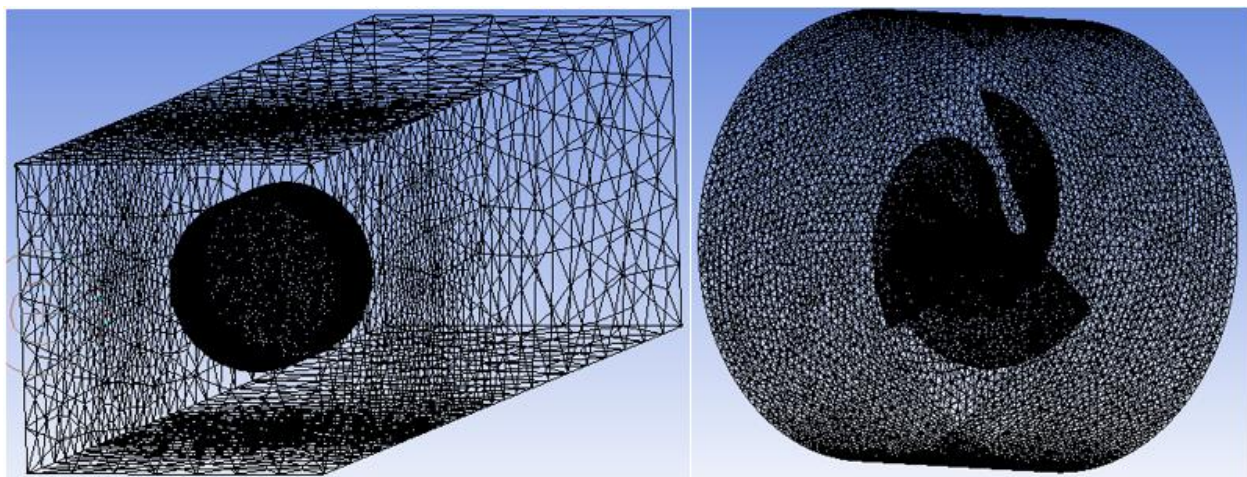
Fig. 4. Two views of the computational meshes of stationary and rotating domains

To ensure mesh-independency of the computational results, careful mesh study was carried out by increasing the number of mesh elements.

Figure 5 shows the mesh tests for the four models of the turbine blades. The tests were carried out by considering the variation of power coefficient (C_p) of the blades with the number of mesh elements. Based on the results of Figure 5, the number of mesh elements was about 1.1 million elements for all models.
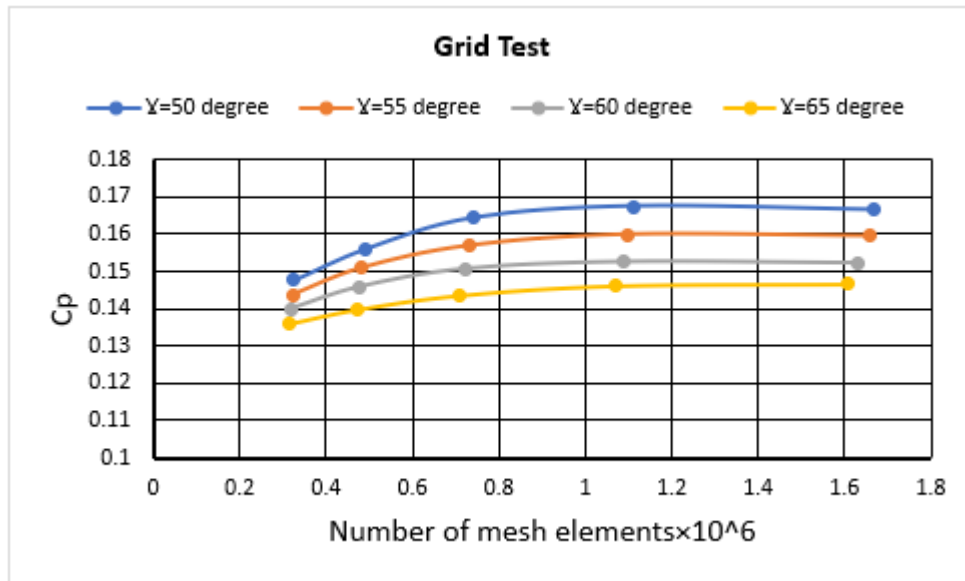
Fig. 5. Mesh test for the four turbine models

In order to accurately predict the flow separation, the SST (Shear Stress Transport) turbulence model was used [9,14,16-18,26,28,36]. The conservative interface flux for mass and momentum was used. The inlet and outlet air flow through the boundary surfaces was automatically calculated. The General Grid Interface (GGI) was used to the three sharing surfaces between stationary and rotating domains [14,16-18,24]. The solution convergence was established by monitoring the residual history and the convergence criterion was 10^{-5} for all variables.

2.2 Experimental Study

As the output power is too small to measure because of the small size of the experimental models, the main objective of the experimental work was to measure the rotating speed of the four turbine models as a performance indicator.

The sizes and configurations of the experimental turbine rotors were the same as those of the computational simulation. Figure 6 shows the four experimental models with the same scale 1/10.

Fig. 6. 3D printed turbine models

To prevent deformation of the blades under the flow stresses, the experimental blades were fabricated by 3D printer with thickness of 3 mm.

The experiments were carried out using a specially designed and fabricated low-speed delivery wind tunnel as shown in Figure 7(a) and 7(b). This tunnel consisted of axial-fan, mechanical gate, transition duct, diffuser, settling chamber, contraction nozzle, and test duct. AC motor (750 W) was used to rotate the axial-fan with a rotational speed of 1360 rpm. The longitudinal centerline of the wind tunnel was above the ground by 78 cm. The outlet cross-sectional area of the wind tunnel was 300×300 mm², which is two times larger than the diameter of the experimental wind-turbine model [15-20]. As shown in Figure 8, the turbine model was placed at the open space at the exit (outlet) of the test duct.

Fig. 7. Two views of the wind tunnel setup

Fig. 8. Wind tunnel and the turbine model

To ensure the flow uniformity at the (exit) outlet of the test duct, velocity measurement was carried out along the two centerlines of the duct cross-section (horizontal and vertical). As can be seen in Figure 9(a), twelve measuring points were distributed along each of the two centerlines. With one measuring point in the center-point of the duct cross-section. Thus, a total number of twenty-

five measuring points were considered. Measuring points were concentrated near the solid walls of the duct to demonstrate the effect of the boundary layer.

The tests were conducted for three different speeds, namely: 5, 8, and 11 m/s to verify the velocity profile with increasing the flow velocity. To measure the velocity values, UT-363 digital manometer [37] was used as shown in Figure 9(b). Figure 10 and 11 illustrate the velocity profiles along the two centerlines in the vertical and horizontal directions, respectively.

It is noticed from both Figure 10 and 11 that the flow profiles of the three velocities are fully-developed and uniform along the most of the vertical and horizontal centerlines in the middle of the open test section; showing a good flow quality with noticeable uniformity.

Normally, the acceptable range of the wind turbine location, for an open-type wind tunnel, from the tunnel exit is between 0.33 and 0.73 times the exit hydraulic diameter [38]. Thus, the present experimental models were placed at 100 mm downstream of the exit of the wind tunnel [15-19].
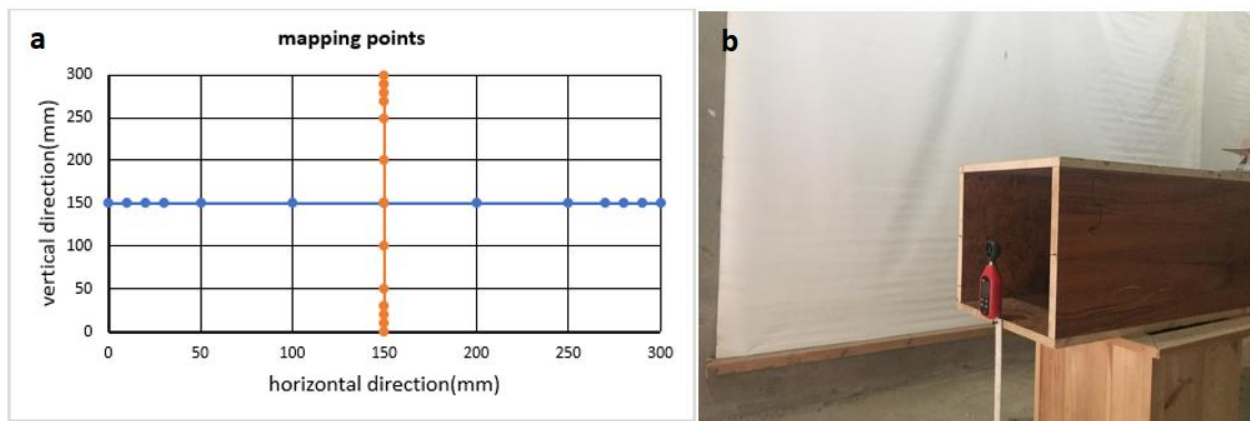

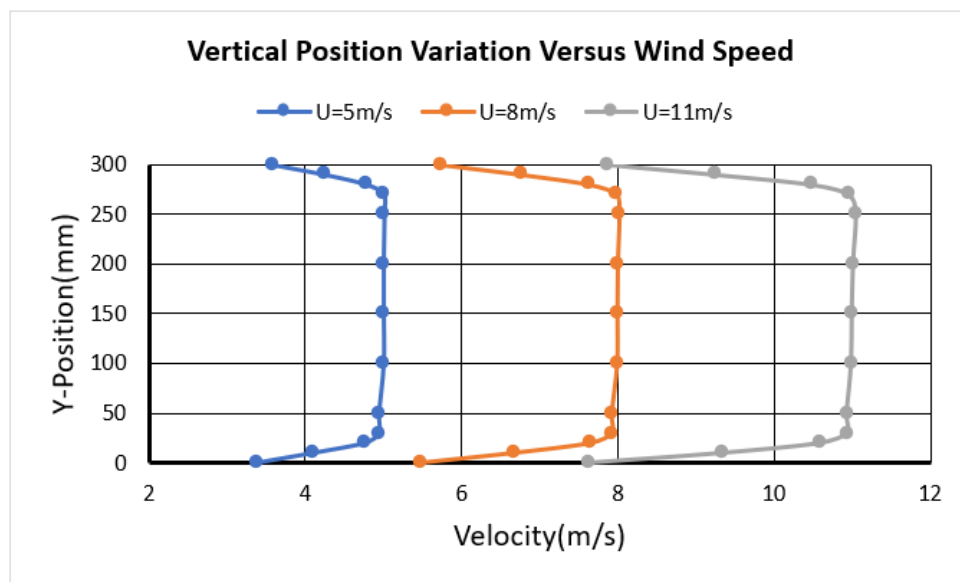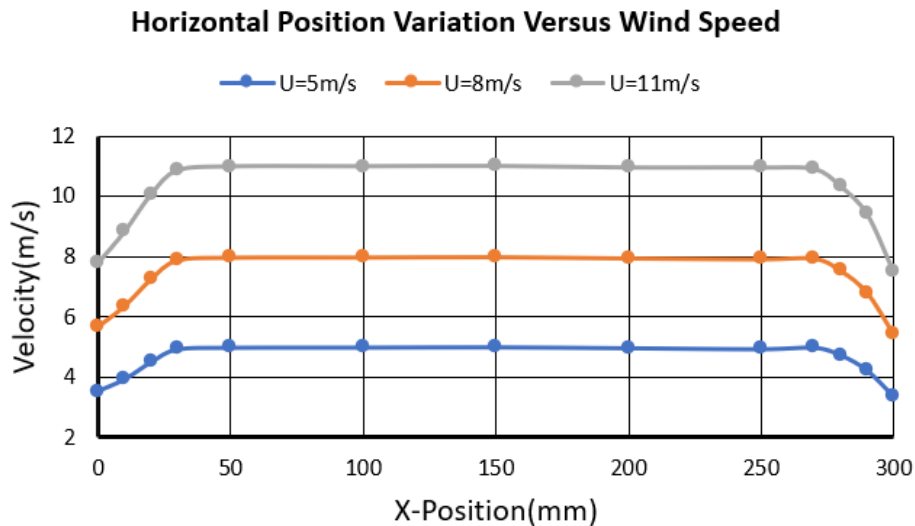**Fig. 9.** (a) Measuring points and (b) Measuring instrument

Fig. 10. Velocity profiles along the centerlines in the vertical direction

**Horizontal Position Variation Versus Wind Speed**

Fig. 11. Velocity profiles along the centerlines in the horizontal direction

For the entire experimentation, the centerline of the turbine model was aligned with the horizontal centerline of the wind tunnel. As can be seen in Figure 6, a single rotating shaft, which was made from Teflon, was used to support each of the four turbines when used in the experimentation. Two roller bearings were used to support the rotating shaft on a suitable metallic base. The rotational speed of the turbine was measured using a non-contact digital tachometer device (UT-373) [39]. This device uses a laser beam which is pointed at a refractor sheet. This sheet refracts the laser beam, which is monitored by an optical sensor, at every rotation. The tachometer was located outside the test section at a fixed location for the whole study, Figure 8. The refractor sticker was attached to the wind turbine shaft to reduce the experimental error.

2.3 Computational Validation

Figure 12 shows the variation of torque coefficient with tip-speed ratio (TSR) for the present investigated down-scale 50°-blade angle model in comparison to the results of Lu [14]. The results of Lu [14] were based on both a steady-state numerical investigation and a theoretical study based on angular momentum equation for the full-scale model.
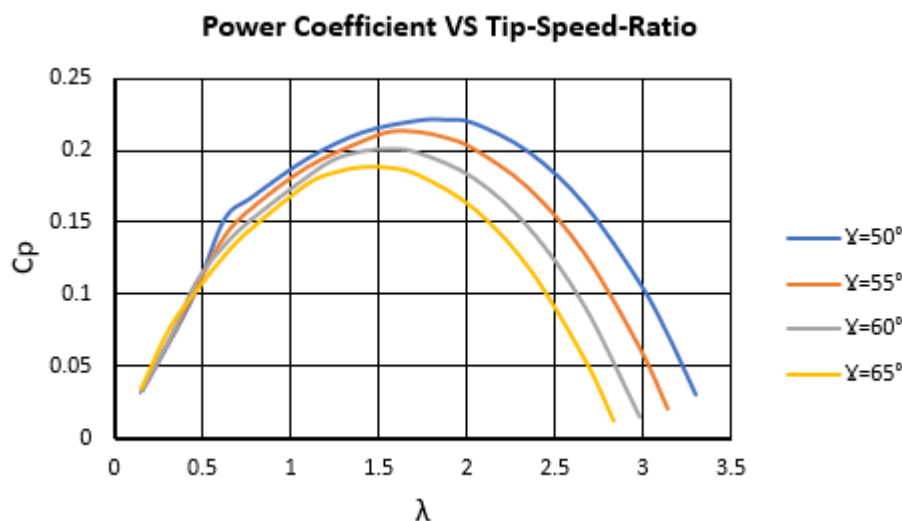
Tip-Speed-Ratio VS Torque Coefficient
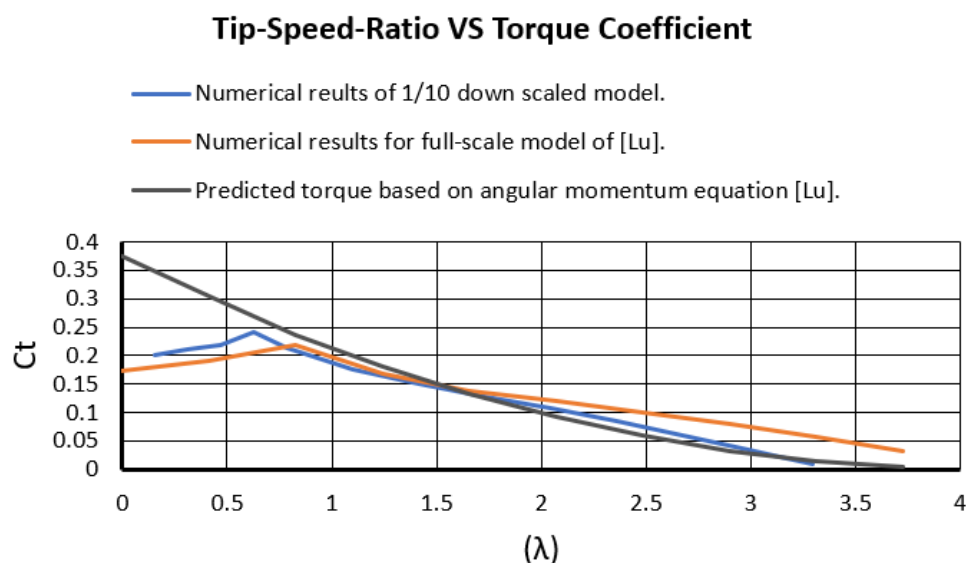
Fig. 12. Computational validation with Lu [1]

Generally, as demonstrated in Figure 12, the values of the torque coefficient (C_t) decrease with the tip-speed ratio (TSR) for both the present results and those of Lu [14]. However, there is a noticeable discrepancy between the two computational/numerical results and the theoretical results at the smallest values of tip-speed ratio till TSR approaches 1.0. Both computational results are in a good agreement with the theoretical torque coefficient from TSR=1 to 2. At relatively high tip-speed ratio (TSR>2), the present computational results of the down-scale model are closer to the theoretical values of the torque coefficient than results of Lu [14].Thus, the good agreement of the present computational results with the theoretical model of Lu [14], for most of the values of TSR, gives worthy confidence in the present computational method.

3. Results and Discussion
3.1 Computational Results

Figure 13 shows the variation of the power coefficient (C_p) with the tip-speed ratio for the four turbine models. As can be seen in Figure 13, the power coefficient decreases with the increase of the blade angle (γ). The 50°-model has the highest power coefficient (C_p) of 0.22 at TSR 1.72, which is larger than the highest power coefficient of 55°-model by 3.5%.
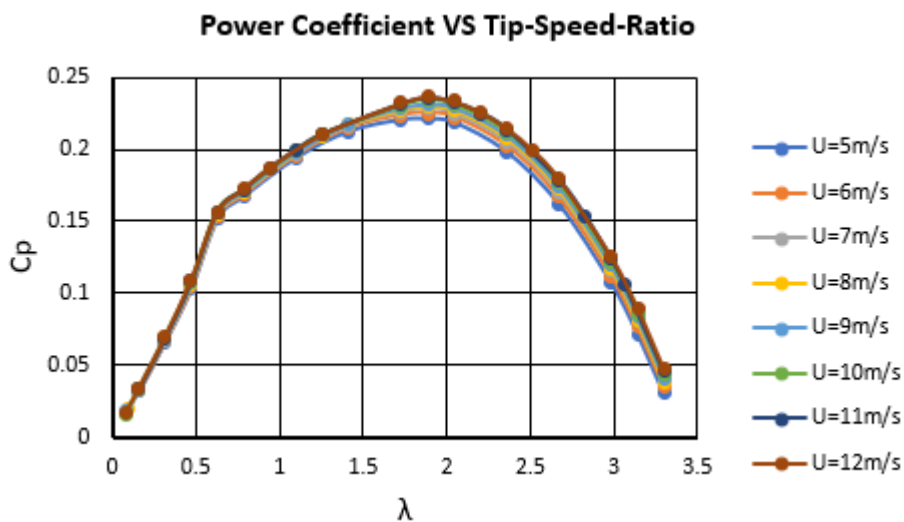

Fig. 13. Variation of power coefficient (C_p) with tip-speed-ratio for the four turbine models

Figure 14 shows the variation of the torque coefficient (C_t) with respect to the tip-speed ratio (λ) for the four turbine models. It is clear that, for the smallest values of TSR (< 0.7), C_t values increase with TSR for the four models. Then, for bigger values of TSR (> 0.7), C_t values decrease with TSR for the four models. The maximum torque coefficient (0.24) is for the 50°-model at TSR 0.62. However, for bigger values of TSR (> 0.7), the values of C_t decrease with the increase of the blade angle (γ).

Figure 15 and 16 show the variation of power coefficient (C_p) and torque coefficient (C_t), respectively, with the tip-speed ratio (λ) for the 50°-model at wind speeds from 5 to 12 m/s by an interval of 1 m/s. As expected, there is no noticeable difference in aerodynamic performance with changing the wind speed for the same model.
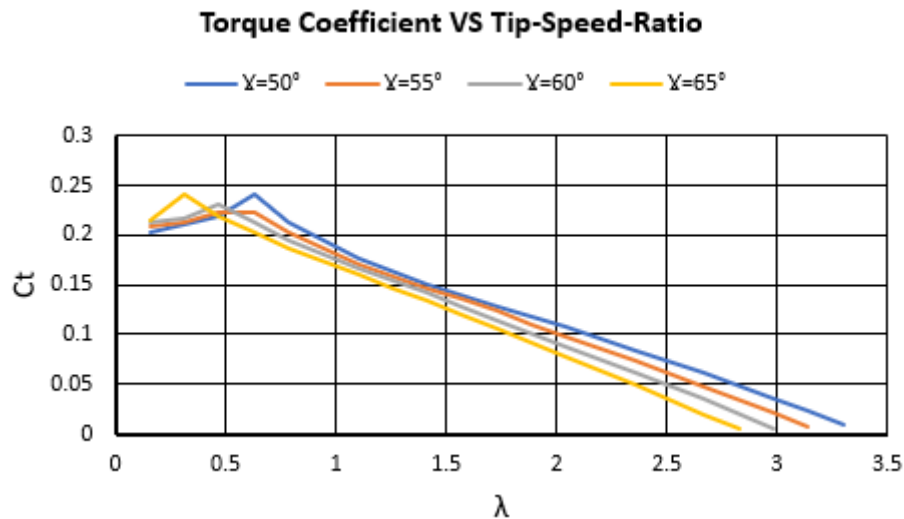
Torque Coefficient VS Tip-Speed-Ratio

Fig. 14. Variation of torque coefficient (C_t) with tip-speed ratio for the four turbine models

Power Coefficient VS Tip-Speed-Ratio

Fig. 15. Variation of power coefficient (Cp) with tip-speed ratio (λ) of 50°-model

Torque Coefficient VS Tip-Speed-Ratio
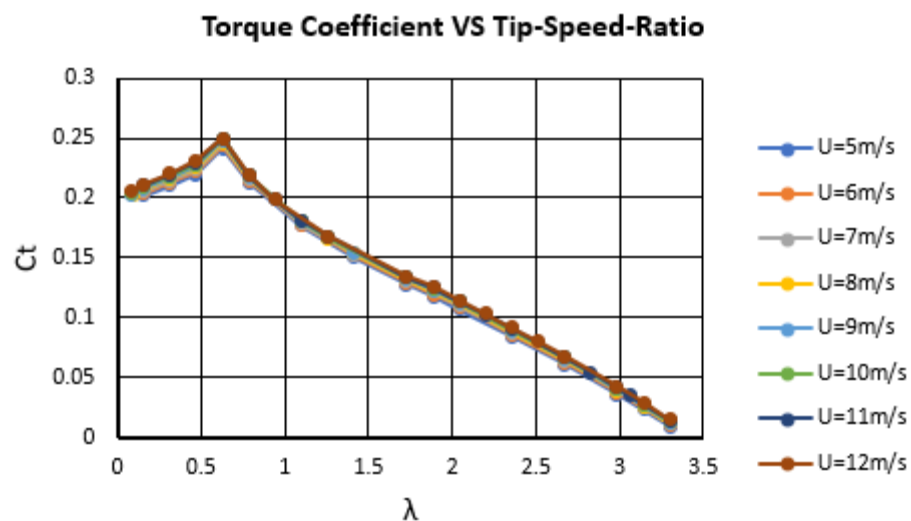
**Fig. 16.** Variation of torque coefficient (C_t) with tip-speed ratio (λ) of 50°-model

3.2 Experimental Results

Table 1 shows the maximum rotating speed, N (rpm), for the four different models at wind speeds from 5 to 12 m/s with an interval of 1 m/s. The measurements were taken for the free-run mode (without load). A graphical presentation of the results of Table 1 is shown in Figure 17.

Table 1
Variation of maximum rotating speed, N (rpm), with wind speed for the four different models

Turbine model	Wind speed (m/s)							
	5	6	7	8	9	10	11	12
50°	196	415	689	790	1173	1354	2376	2913
55°	187	396	657	753	1118	1290	2263	2775
60°	177	376	624	715	1062	1225	2149	2636
65°	167	356	591	677	1006	1160	2035	2497
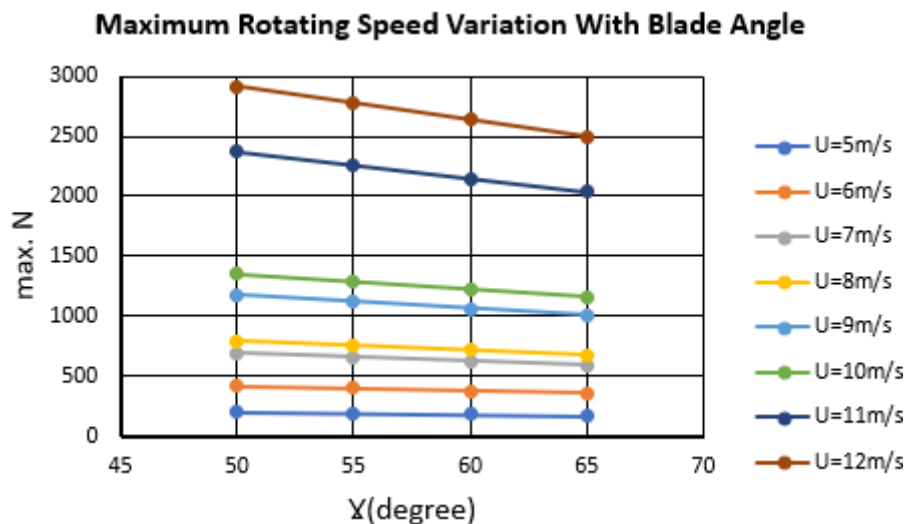
Fig. 17. Variation of maximum rotating speed, N (rpm), with wind speed for the four different models

Based on Table 1 and Figure 17, it can be stated that the maximum rotating speed for the 50°-model at the designed wind-speed (5 m/s) is 196 rpm, and at the maximum wind speed (12 m/s) is 2,913 rpm. The maximum rotating speed decreases with the increase of the blade angle, which indicates an expected increase of the output power at low blade angles.

4. Conclusions

The present computational study demonstrates the variation of the Archimedes wind-turbine performance (power and torque coefficients) with the blade angle. The computational investigation covered wind speeds from 5 to 12 m/s with an interval of 1 m/s. The blade angle was changed from 50° to 65°.

Due to the very small output-power of the present experimental models, the values of the maximum rotational speed were considered as an indication of the turbine performance.

Based on the above results and discussions, maximum power coefficient (C_p) is 0.22 at TSR=1.72, which is for the 50°-model. Maximum torque coefficient (C_t) is 0.24 at TSR = 0.62, which is for the 50°-model. At the lowest tip-speed ratio (TSR), the Archimedes wind turbine has the unusual behavior of

increasing torque with the increase of TSR. This behavior needs more full-scale experimental investigation for better explanation.

The maximum rotational speed of the down-scale turbine model is 196 rpm at wind speed 5m/s, which corresponds to TSR=0.3.

Archimedes wind turbine has the greatest power coefficient (C_p) at the lower tip-speed ratios in comparison to Savonious turbines, which makes Archimedes wind turbine perfect for urban environment.

References

[1] Paraschivoiu, Ion, Sami Ammar, and Farooq Saeed. "VAWT versus HAWT: a comparative performance study of 2–6 MW rated capacity turbines." *Transactions of the Canadian Society for Mechanical Engineering* 42, no. 4 (2018): 393-403. https://doi.org/10.1139/tcsme-2017-0137

[2] Johari, M., Muhd Jalil, and Mohammad Faizal Mohd Shariff. "Comparison of horizontal axis wind turbine (HAWT) and vertical axis wind turbine (VAWT)." *International Journal of Engineering and Technology* 7, no. 4.13 (2018): 74-80. https://doi.org/10.14419/ijet.v7i4.13.21333

[3] Pope, K., I. Dincer, and G. F. Naterer. "Energy and exergy efficiency comparison of horizontal and vertical axis wind turbines." *Renewable energy* 35, no. 9 (2010): 2102-2113. https://doi.org/10.1016/j.renene.2010.02.013

[4] Galinos, Christos, Torben J. Larsen, Helge Aagaard Madsen, and Uwe Schmidt Paulsen. "Vertical axis wind turbine design load cases investigation and comparison with horizontal axis wind turbine." *Energy Procedia* 94 (2016): 319-328. https://doi.org/10.1016/j.egypro.2016.09.190

[5] Govind, Bala. "Increasing the operational capability of a horizontal axis wind turbine by its integration with a vertical axis wind turbine." *Applied Energy* 199 (2017): 479-494. https://doi.org/10.1016/j.apenergy.2017.04.070

[6] Khaled, Mohamed, Mostafa M. Ibrahim, Hesham E. Abdel Hamed, and Ahmed F. AbdelGwad. "Investigation of a small Horizontal–Axis wind turbine performance with and without winglet." *Energy* 187 (2019): 115921. https://doi.org/10.1016/j.energy.2019.115921

[7] Chen, Yu-Jen, Guo-Yuan Huang, Y. C. Shiah, and Yi-Lun Tsai. "Performance Prediction for Small Horizontal Axis Wind Turbine (HAWT) by Integrated Theory and Experimental Verifications." *International Journal of Precision Engineering and Manufacturing-Green Technology* 7, no. 1 (2020): 131-140. https://doi.org/10.1007/s40684-019-00141-1

[8] Tjahjana, Dominicus Danardono Dwi Prija, Syamsul Hadi, Yoga Arob Wicaksono, Diniar Mungil, Fahrudin Kurniawati, Ilham Satrio Utomo, and Sukmaji Indro Cahyono andAri Prasetyo. "Study on Performance Improvement of the Savonius Wind Turbine for Urban Power System with Omni-directional Guide Vane (ODGV)." *Journal of Advanced Research in Fluid Mechanics and Thermal Sciences* 55, no. 1 (2019): 126-135.

[9] Jang, Hyeonmu, Insu Paek, Seungjoo Kim, and Deockjin Jeong. "Performance Prediction and Validation of a Small-Capacity Twisted Savonius Wind Turbine." *Energies* 12, no. 9 (2019): 1721. https://doi.org/10.3390/en12091721

[10] Loganathan, Bavin, Harun Chowdhury, Israt Mustary, and Firoz Alam. "An experimental study of a cyclonic vertical axis wind turbine for domestic scale power generation." *Procedia Engineering* 105 (2015): 686-691. https://doi.org/10.1016/j.proeng.2015.05.057

[11] Gürbüz, M. Tayyip, Menal İlhan, Sercan Acarer, and Z. Haktan Karadeniz. "Investigation of radial turbines for wind energy harvesting." *Proceedings of the Institution of Mechanical Engineers, Part A: Journal of Power and Energy* 233, no. 5 (2019): 659-672. https://doi.org/10.1177/0957650919861615

[12] Acarer, Sercan, Çağlar Uyulan, and Ziya Haktan Karadeniz. "Optimization of radial inflow wind turbines for urban wind energy harvesting." *Energy* (2020): 117772. https://doi.org/10.1016/j.energy.2020.117772

[13] Ji, HoSeong, Kyung Chun Kim, Joon Ho Baek, and R. R. Ruijtenbeek. "The aerodynamic method of the Archimedes Windturbine." *Journal of Power Solutions* (2014).

[14] Lu, Qian, Qiang Li, Yoon-Kee Kim, and Kyung-Chun Kim. "A study on design and aerodynamic characteristics of a spiral-type wind turbine blade." *Journal of the Korean society of visualization* 10, no. 1 (2012): 27-33. https://doi.org/10.5407/JKSV.2011.10.1.027

[15] Safdari, Arman, and Kyung Chun Kim. "Aerodynamic and structural evaluation of horizontal archimedes spiral wind turbine." *Journal of Clean Energy Technologies* 3, no. 1 (2015): 34-38. https://doi.org/10.7763/JOCET.2015.V3.164

[16] Kim, Kyung Chun, Ho Seong Ji, Yoon Kee Kim, Qian Lu, Joon Ho Baek, and Rinus Mieremet. "Experimental and numerical study of the aerodynamic characteristics of an archimedes spiral wind turbine blade." *Energies* 7, no. 12 (2014): 7893-7914. https://doi.org/10.3390/en7127893

[17] Kim, Kyung Chun, Yoon Kee Kim, Ho Seong Ji, Jook Ho Beak, and Rinus Mieremet. "Aerodynamic Characteristics of Horizontal Axis Wind Turbine With Archimedes Spiral Blade." In *ASME International Mechanical Engineering Congress and Exposition*, vol. 56321, p. V07BT08A070. American Society of Mechanical Engineers, 2013. https://doi.org/10.1115/IMECE2013-62734

[18] Kim, Yoon Kee, Qian Lu, Ho Seong Ji, Joon Ho Beak, Rinus Mieremet, and Kyung Chun Kim. "A multi-prong study on aerodynamic characteristics of archimedes spiral-type wind turbine blade." *Energies* (2014). https://doi.org/10.3390/en7127893

[19] Ji, Ho Seong, Li Qiang, Joon Ho Beak, Rinus Mieremet, and Kyung Chun Kim. "Effect of the wind direction on the near wake structures of an Archimedes spiral wind turbine blade." *Journal of Visualization* 19, no. 4 (2016): 653-665. https://doi.org/10.1007/s12650-016-0356-8

[20] Li, Qiang, Hyun Dong Kim, Ho Seong Ji, and Kyung Chun Kim. "Flow Characteristics Around Archimedes Wind Turbine according to the Change of Angle of Attack." *Journal of the Korean Society of Visualization* 11, no. 1 (2013): 28-33. https://doi.org/10.5407/JKSV.2013.11.1.028

[21] Yang, Sung-Moon, Ho-Seong Ji, Do-Sik Shim, Joon-Ho Baek, and Sang-Hu Park. "Conical roll-twist-bending process for fabrication of metallic archimedes spiral blade used in small wind power generator." *International Journal of Precision Engineering and Manufacturing-Green Technology* 4, no. 4 (2017): 431-439. https://doi.org/10.1007/s40684-017-0048-4

[22] Ji, Ho Seong, Joon Ho Baek, Rinus Mieremet, and Kyung Chun Kim. "The Aerodynamic Performance Study on Small Wind Turbine with 500W Class through Wind Tunnel Experiments." *International Journal of Renewable Energy Sources* 1 (2016): 7-12.

[23] H. Ji, J. Baek, R. Mieremet, and K. C. Kim. "Aerodynamic characteristics of an Archimedes spiral wind turbine blade according to the angle of attack change." In *Europe's premier wind energy event*, Barcelona, Spain (2014).

[24] Chaudhary, Shashank, Shubham Jaiswal, Richa Nanda, S. Patel, and P. Kumar. "Comparison of torque characteristics of Archimedes wind turbine evaluated by analytical and experimental study‖." *International Journal of Mechanical and Production Engineering* 4, no. 8 (2016): 75-78.

[25] D. S. Sandeep, K. V. Krunal, R. Karishma, C. Ravikumar, and R. P. Y. Deepak. "Design, fabrication and aerodynamic analysis of a modified Archimedes wind turbine." *International Journal of Research and Scientific Innovation (IJRSI)* (2017).

[26] Rao, S. Srinivasa, Kota Shanmukesh, M. K. Naidu, and Praveen Kalla. "Design and Analysis of Archimedes Aero-Foil Wind Turbine Blade for Light and Moderate Wind Speeds." *International Journal on Recent Technologies in Mechanical and Electrical Engineering* 5, no. 8 (2018): 01-05.

[27] Ebrahimi, Sahand, and Mohammad Aref Ghassemi. "Numerical aerodynamics analysis of the of the Archimedes screw wind turbine." *Int. J Multidisciplinary Sci & Eng* (2018): 12-15.

[28] Jang, Hyeonmu, Dongmyeong Kim, Yechan Hwang, Insu Paek, Seungjoo Kim, and Joonho Baek. "Analysis of Archimedes Spiral Wind Turbine Performance by Simulation and Field Test." *Energies* 12, no. 24 (2019): 4624. https://doi.org/10.3390/en12244624

[29] J. H. Baek, B. S. Kim, S. k. Min, and M. Mieremet. "Spiral blade unit and wind generator." *W.I.P. Organization* (2017).

[30] Rozaim, Muhammad Faiz, Fazila Mohd Zawawi, Nur Safwati Mohd Nor, Haslinda Mohamed Kamar, and Nazri Kamsah. "Experimental study on performance of low speed wind turbine for application in Malaysia." *Journal of Advanced Research in Fluid Mechanics and Thermal Sciences* 26, no. 1 (2016): 20-28.

[31] Majunit, Nurul Izyan, Fazila M. Zawawi, Nur Safwati Mohd Nor, Haslinda Mohamed Kamar, and Nazri Kamsah. "Numerical investigation of vortex formation effect on horizontal axis wind turbine performance in low wind speed condition." *Journal of Advanced Research In Fluid Mechanics And Thermal Sciences* 27, no. 1 (2016): 1-11.

[32] Gahraz, Seyed Reza Jafari, Tholudin Mat Lazim, and Masoud Darbandi. "Wind Tunnel Study of the Effect Zigzag Tape on Aerodynamics Performance of A Wind Turbine Airfoil." *parameters* 41, no. 1 (2018): 1-9.

[33] Khanjari, Ali, Esmail Mahmoodi, and Mohammad Hossien Ahmadi. "Energy and exergy analyzing of a wind turbine in free stream and wind tunnel in CFD domain based on actuator disc technique." *Renewable Energy* (2020). https://doi.org/10.1016/j.renene.2020.05.183

[34] Xu, Zhang, Yan-Hao Feng, Chuang-Yao Zhao, Yu-Lei Huo, Sha Li, Xiao-Jian Hu, and Ying-Jie Zhong. "Experimental and numerical investigation on aerodynamic performance of a novel disc-shaped wind rotor for the small-scale wind turbine." *Energy Conversion and Management* 175 (2018): 173-191. https://doi.org/10.1016/j.enconman.2018.09.003

[35] Van Bussel, G. J. W., S. Mertens, H. Polinder, and H. F. A. Sidler. "TURBY®: concept and realisation of a small VAWT for the built environment." In *Proceedings of the EAWE/EWEA Special Topic conference" The Science of making Torque from Wind", Delft, The Netherlands*. 2004.

[36] Cao, Han. "Aerodynamics analysis of small horizontal axis wind turbine blades by using 2D and 3D CFD modelling." PhD diss., University of Central Lancashire, 2011.

[37] Uni-Trend. " UT363 Mini Anemometer".

[38] Ewald, B. F. *Wind Tunnel Wall Corrections (la Correction des effets de paroi en soufflerie)*. No. AGARD-AG-336. Advisory Group For Aerospace Research And Development Neuilly-Sur-Seine (France), 1998.

[39] Uni-Trend. " UT373 Mini Tachometer".